

Light-by-light scattering in the Lamb shift and the bound electron g factor

Andrzej Czarnecki¹ and Robert Szafron ^{a1}

¹*Department of Physics, University of Alberta, Edmonton, Alberta, Canada T6G 2G7*

We compute an $\mathcal{O}(\alpha^2(Z\alpha)^6)$ contribution to the hydrogen-atom Lamb shift arising from the light-by-light scattering. Analogous diagrams, with one atomic electric field insertion replaced by an external magnetic field, contribute to the gyromagnetic factor of the bound electron at $\mathcal{O}(\alpha^2(Z\alpha)^4)$. We also calculate the contribution to the gyromagnetic factor from the muon magnetic loop.

I. INTRODUCTION

Light-by-light scattering (LBL) arises when a virtual charged particle induces an interaction among photons. Because of the charge conjugation symmetry of quantum electrodynamics (QED), the number n_γ of the coupled photons must be even [1]. When $n_\gamma = 4$, a number of phenomena result that manifest themselves, for example, by a slight change of energy levels in hydrogen. Averaged over possible spin orientations of the electron and the proton, this constitutes a part of the Lamb shift.

Examples of possible processes are shown in Fig. 1. Fig. 1(a) shows the lowest order contribution of the so-called

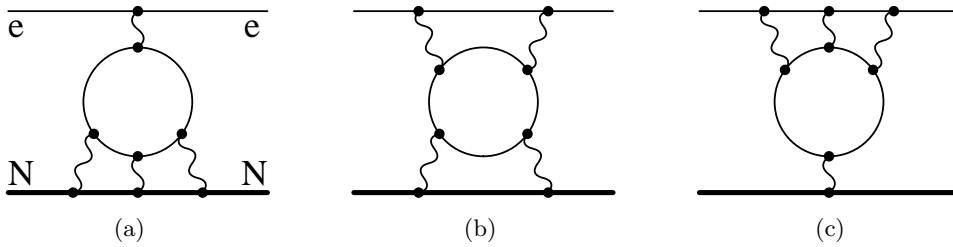


FIG. 1. Examples of light-by-light scattering contributions to the Lamb shift. Thin lines denote electrons and the thick one is the nucleus.

Wichmann-Kroll potential, first considered in [2, 3]. Its effect is $\mathcal{O}(\alpha(Z\alpha)^6)$ and shifts the 1S level of hydrogen ($Z = 1$) by 2.5 kHz. For comparison, the total Lamb shift of the 1S level starts at $\mathcal{O}(\alpha(Z\alpha)^4 \ln Z\alpha)$ and is about 8 MHz (for a review of the theory of the Lamb shift see [4]).

Fig. 1(b) is an example of an $\mathcal{O}(\alpha^2(Z\alpha)^5)$ effect. Such LBL effects were computed in [5–7] and confirmed in [8]; they shift the 1S level by -5.3 kHz.

Finally, Fig. 1(c) is an $\mathcal{O}(\alpha^3(Z\alpha)^4)$ LBL contribution to the Lamb shift that enters through the slope of the Dirac form factor computed at this order in [9].

A peculiarity of atomic physics is that a given QED Feynman diagram gives rise to contributions at various orders in $Z\alpha$. In this paper, we determine the effect of diagrams similar to Fig. 1(b) in the next order in the $Z\alpha$ expansion, $\mathcal{O}(\alpha^2(Z\alpha)^6)$. Effects related to the self-energy of the electron at this order were studied in [10], but the LBL contribution was not included there.

Of course, attaching an extra photon to the electron loop would give zero because of the Furry theorem [1]. Instead, we consider a different region of momenta $\mathbf{q}_{1,2}$ of the two photons exchanged between the nucleus and the electron loop (“Coulomb photons”).

It is convenient to classify effects of photon exchanges according to how the momentum they carry scales with the atomic number Z . Results $\mathcal{O}(\alpha^2(Z\alpha)^5)$ are obtained when the Coulomb photons are hard, $|\mathbf{q}_i| \sim m_e \gg m_e Z\alpha$. They scale like the momentum inside the LBL loop that is of the order of m_e (there is no dependence on Z). In this case, the momentum transferred between the electron and the nucleus (that scales like $Z\alpha m_e$) can be neglected. This gives rise to a contact interaction between the electron and the nucleus, as shown in the upper panel of Fig. 2. This interaction creates an effective potential proportional to $(Z\alpha)^2 \delta^3(\mathbf{r})$ [11, 12], scaling with the nuclear charge as $\sim (Z\alpha)^5$ and contributing to the Lamb shift at $\mathcal{O}(\alpha^2(Z\alpha)^5)$.

In this paper, we consider instead a situation where both Coulomb photons carry a small momentum, $\vec{q}_i \ll m_e$. Then the LBL loop can be expanded in \mathbf{q}_i . The leading term in this expansion is proportional to $(Z\alpha)^2 \frac{\mathbf{q}_1 \cdot \mathbf{q}_2}{\mathbf{q}_1^2 \mathbf{q}_2^2}$ [10, 13].

^a Present address: Physik Department T31, James-Franck-Str. 1, Technische Universität München, D85748 Garching, Germany

The resulting interaction is illustrated in the lower panel of Fig. 2. In position space this term is proportional to the square of the electric field \mathbf{E}^2 . Since the electric field scales as $\sim Z\alpha/r^2 \sim (Z\alpha)^3$, this contribution is $\mathcal{O}(\alpha^2(Z\alpha)^6)$.

The corresponding effect on the Lamb shift is presented in Section II. An analogous effect on the bound-electron gyromagnetic factor (g) is described in Section III.

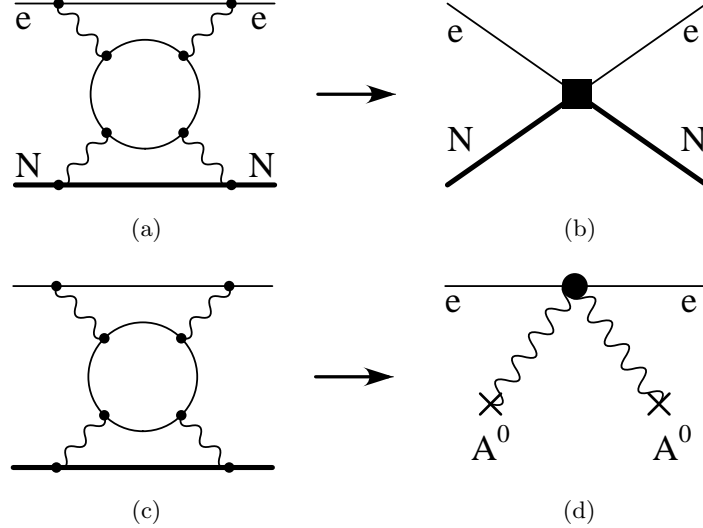


FIG. 2. Matching with all photons hard (upper panel). Here, Coulomb photons are part of short-distance loops (a) that can be matched onto a point interaction (b). When the Coulomb field carries soft momentum (lower panel), the remaining two short-distance loops in (c) are shrunk into an effective vertex connecting two electron fields and two Coulomb photons (d). This results in corrections $\mathcal{O}((Z\alpha)^6)$.

II. LBL CONTRIBUTION TO THE LAMB SHIFT AT $\mathcal{O}(\alpha^2(Z\alpha)^6)$

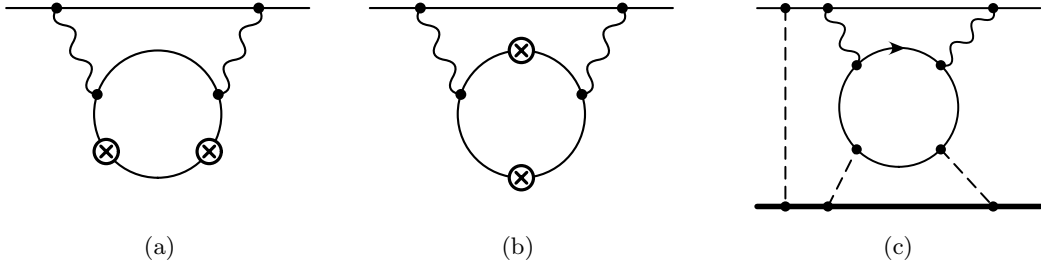


FIG. 3. Light-by-light scattering contributions to the Lamb shift. Crosses in (a) and (b) denote couplings of the electric field photons in whose momenta we expand. (c): an example of a hard-momentum diagram which cancels the logarithmic divergence induced by (a) and (b).

The contribution of diagrams in Fig. 3(a,b) to the scattering amplitude T of an electron on an electric field [10] is found by computing two-loop integrals with the result

$$\Delta T_{\text{LBL}} = \chi_{\text{LBL}} \mathbf{q}_1 \cdot \mathbf{q}_2, \quad (1)$$

$$\chi_{\text{LBL}} = \frac{43}{144} - \frac{133}{3456} \pi^2, \quad (2)$$

where $\mathbf{q}_{1,2}$ denote the momenta of the Coulomb photons in Fig. 2(d). The effective operator induced by the diagrams in Fig. 3 is proportional to the square of the electric field [10], $\mathbf{E}^2 \sim 1/r^4$. The expectation value of this operator in the hydrogen ground state has an ultraviolet divergence. In momentum space $r^{-4} \rightarrow k$, while the Fourier transform of the charge density behaves at large k as $1/k^4$. Altogether, the expectation value behaves like $\int \frac{k^3 k}{k^4}$, and diverges logarithmically.

This divergence is canceled by other diagrams, such as shown in Fig. 3(c), where all photons are hard. In the sum of all contributions only a logarithm of the ratio of scales survives. Its contribution to the nS energy levels is

$$\Delta E_n = \left(\frac{\alpha}{\pi}\right)^2 \frac{(Z\alpha)^6}{n^3} \ln(Z\alpha)^2 \cdot 4\chi_{\text{LBL}}. \quad (3)$$

For example, the $1S$ - $2S$ energy splitting in hydrogen ($Z = 1$) is decreased by about 280 Hz. For comparison, the experimental uncertainty is just 10 Hz [14].

The $1S$ - $2S$ splitting is also of experimental interest in the hydrogen-like helium ion He^+ ($Z = 2$) [15, 16]. The correction we have found reduces that splitting by a much larger amount, 15.5 kHz.

The effect we have found modifies the so-called coefficient B_{61} [10, 17] in front of the term $\mathcal{O}(\alpha^2(Z\alpha)^6 \ln(Z\alpha)^{-2})$. The total linear logarithmic contribution to the ground state energy in this order becomes

$$\Delta E_{1S} = \left(\frac{\alpha}{\pi}\right)^2 (Z\alpha)^6 \ln(Z\alpha)^{-2} \left[\frac{413581}{64800} + \frac{4}{3}N(1S) + \frac{2027}{864}\pi^2 - \frac{616}{135}\ln(2) \right. \\ \left. - \frac{2}{3}\pi^2\ln(2) + \frac{40}{9}\ln^2(2) + \zeta(3) + \left(-\frac{43}{36} + \frac{133}{864}\pi^2\right)_{\text{LBL}} \right], \quad (4)$$

where $N(1S)$ was calculated in [17]. The operator \mathbf{E}^2 contributes also to the normalized difference of expectation values for S states considered in [10],

$$\left\langle \left\langle \frac{(Z\alpha)^2}{r^4} \right\rangle \right\rangle = n^3 \left\langle nS \left| \frac{(Z\alpha)^2}{r^4} \right| nS \right\rangle - \left\langle 1S \left| \frac{(Z\alpha)^2}{r^4} \right| 1S \right\rangle \quad (5)$$

$$= 8(Z\alpha)^6 \left[H_n - \ln n - \frac{2}{3} - \frac{1}{2n} + \frac{1}{6n^2} \right]; \quad (6)$$

where $H_n = \sum_{k=1}^n \frac{1}{k}$ are harmonic numbers. Hence, this observable is also changed by our additional contribution to the coefficient of $1/r^4$ in Eq. (2) (see Eq. (2.10) in [10]).

III. THE g FACTOR OF A BOUND ELECTRON

When one of the Coulomb photons in Fig. 3(a,b) is replaced by an external magnetic field, we obtain an effective interaction contributing to the bound electron g -factor, as shown in Fig. 4. Momenta in both loops are on the order

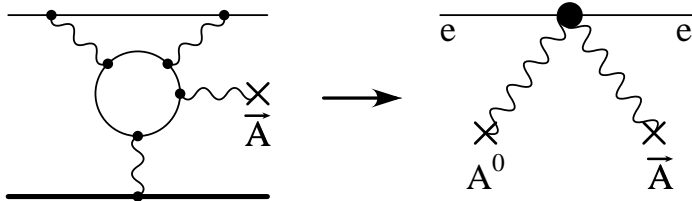


FIG. 4. The LBL contribution to the bound electron g -factor is shrunk to a point interaction. The effective vertex contains two different operators, see text.

of the electron mass and the loops can be treated as short-distance processes, compared with the size of the atom. They induce effective low energy operators, like in the case of the Lamb shift. We depict the matching procedure in Fig. 4. Two low-energy operators [18] contribute to the effective vertex,

$$\delta V = \frac{e^2}{2m} (2\eta\sigma^{ij}B^{ik}\nabla^j E^k + \xi\sigma^{ij}B^{ij}\nabla^k E^k). \quad (7)$$

Here we use a d -dimensional notation ($d = 3 - 2\epsilon$), $\sigma^{ij} = \frac{1}{2i}[\sigma^i, \sigma^j]$ and $B^{ij} = \nabla^i A^j - \nabla^j A^i$. The two terms in (7) differ only by the contraction of vector indices. In an S -state only scalar averages of both operators contribute. The $\mathcal{O}(\alpha^2)$ correction to the g -factor due to the LBL contribution in an S -state is, in the limit $d \rightarrow 3$,

$$g_{\text{LBL}}^{(2)} = 16(Z\alpha)^4 \left(\frac{2}{3}\eta + \xi \right). \quad (8)$$

We find that diagrams of the type shown in Fig. 4 contribute $\Delta\eta = \left(\frac{\alpha}{4\pi}\right)^2 \left(\frac{31}{72}\pi^2 - \frac{22}{9}\right)$ and $\Delta\xi = \left(\frac{\alpha}{4\pi}\right)^2 \left(\frac{16}{9} - \frac{25}{54}\pi^2\right)$, giving

$$g_{\text{LBL}}^{(2)} = (Z\alpha)^4 \left(\frac{\alpha}{\pi}\right)^2 \frac{16 - 19\pi^2}{108}. \quad (9)$$

For completeness let us show the total contribution to parameters ξ and η at the order α^2 , including previously calculated vacuum polarization and self-energy diagrams [18]

$$\eta = \left(\frac{\alpha}{4\pi}\right)^2 \left[\left(\frac{2528}{81} - \frac{169}{54}\pi^2\right)_{\text{VP}} + \left(\frac{31}{72}\pi^2 - \frac{22}{9}\right)_{\text{LBL}} - \frac{283}{10} + \frac{169}{120}\pi^2 - \frac{4}{15}\pi^2 \ln 2 + \frac{2}{5}\zeta(3) - \frac{16}{3\varepsilon} \right], \quad (10)$$

$$\xi = \left(\frac{\alpha}{4\pi}\right)^2 \left[\left(\frac{2674}{81} - \frac{91}{27}\pi^2\right)_{\text{VP}} + \left(\frac{16}{9} - \frac{25}{54}\pi^2\right)_{\text{LBL}} - \frac{152}{15} + \frac{319}{45}\pi^2 - \frac{68}{5}\pi^2 \ln 2 + \frac{102}{5}\zeta(3) + \frac{4}{3\varepsilon} \right]. \quad (11)$$

For the 1S state, the total correction to the g -factor including the LBL contribution is

$$g^{(2)} \approx (Z\alpha)^4 \left(\frac{\alpha}{\pi}\right)^2 \left[-18.03 - \frac{56}{9} \ln Z\alpha \right]. \quad (12)$$

The total correction of the order $\left(\frac{\alpha}{\pi}\right)^2 (Z\alpha)^4$, including the light-by-light contribution becomes

$$g^{(2)} = \left(\frac{\alpha}{\pi}\right)^2 \frac{(Z\alpha)^4}{n^3} \left\{ \frac{28}{9} \ln[(Z\alpha)^{-2}] + \frac{258917}{19440} - \frac{4}{9} \ln k_0 - \frac{8}{3} \ln k_3 + \frac{113}{810}\pi^2 - \frac{379}{90}\pi^2 \ln 2 + \frac{379}{60}\zeta(3) \right. \\ \left. + \left(\frac{16 - 19\pi^2}{108}\right)_{\text{LBL}} + \frac{1}{n} \left[-\frac{985}{1728} - \frac{5}{144}\pi^2 + \frac{5}{24}\pi^2 \ln 2 - \frac{5}{16}\zeta(3) \right] \right\}, \quad (13)$$

where k_0 and k_3 are Bethe-logarithms defined and calculated in [18].

Measurements of the bound g -factor are the best current source of the electron atomic mass [19]. Since corrections $\mathcal{O}(\alpha^2(Z\alpha)^5)$ are not yet known, data with various values of Z are used to fit them. In this approach, also the sensitivity to the presently found LBL effects is diminished. Once the $\mathcal{O}(\alpha^2(Z\alpha)^5)$ corrections become available, an analogous fit will be used to constrain even higher order effects and further improve the knowledge of the electron mass. Then our $\mathcal{O}(\alpha^2(Z\alpha)^4)$ LBL result will allow for a reliable result.

A contribution to the bound-electron g -factor can also be obtained from diagrams in Fig. 3(a,b) by replacing one of the photons connecting the electron line to the LBL loop by an external magnetic field. This results in an effect $\mathcal{O}(\alpha(Z\alpha)^5)$, already evaluated in [20, 21].

IV. MAGNETIC LOOP WITH VIRTUAL MUONS

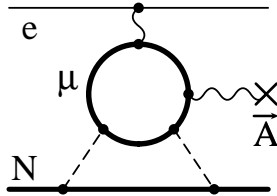


FIG. 5. Magnetic loop with a virtual muon.

Recently [22] the contribution of virtual muon loops to the bound electron g -factor has been computed. Here we reevaluate the magnetic loop, Fig. 5, that on the basis of the results in [22] seems easiest to confirm experimentally among the LBL effects induced by virtual muons. We find its contribution to be

$$g_{\text{ML}}(\text{muon}) = \frac{7}{216}\alpha(Z\alpha)^5 \left(\frac{m_e}{m_\mu}\right)^3. \quad (14)$$

This turns out to be the same as the magnetic loop containing a virtual electron [20, 21], except for the additional factor $(m_e/m_\mu)^3$. With hindsight this is easy to explain. The magnetic interaction in Fig. 5 involves a scattering

of the external magnetic field photon on the virtual muon (that interacts with the nucleus via Coulomb photons indicated by dashed lines) before coupling to the atomic electron. This is an example of the Delbrück scattering. The amplitude of this scattering is inversely proportional to the cube of the virtual fermion mass, a consequence of gauge invariance [20].

Numerically, (14) gives $g_{ML}(\text{muon}) = 5.5 \cdot 10^{-22}$ for hydrogen, $Z = 1$, and $4.3 \cdot 10^{-18}$ for $Z = 6$, the much studied carbon ion. Both numbers are about two orders of magnitude smaller than the values given in [22]. Thus, contrary to the conclusion [22], we believe that the effect of the magnetic muon loop is too small to discern because of nuclear uncertainties.

V. CONCLUSIONS

We have presented new contributions to the Lamb shift and the bound-electron g factor in hydrogen-like systems, arising from the light-by-light scattering.

For the g factor, the new LBL contributions will influence the determination of the electron mass when the $\mathcal{O}(\alpha^2(Z\alpha)^5)$ corrections become available. We also found that the effect of the muon magnetic loop is equal to the analogous effect for the electron loop [20] multiplied by three powers of the electron to muon mass ratio. This simple scaling is valid only for particles whose masses are larger than the inverse atom radius and smaller than the inverse nucleus radius. For light hydrogen-like ions, both the electron and the muon satisfy these conditions but for example the tau lepton does not. For the tau, we expect that the effect will be decreased by the nucleus form-factor effects and further modified by the nuclear recoil.

For the Lamb shift, we have found a new logarithmic effect that decreases the theoretical prediction for the 1S-2S splitting by an amount 28 times larger than the experimental error. This finding strengthens the message of the recent review of the proton radius puzzle [23]: the theory of the hydrogen spectrum has to be further scrutinized and its every aspect should be checked.

ACKNOWLEDGMENTS

We thank Z. Harman, R. Pohl, and V. A. Yerokhin for useful comments. This research was supported by Natural Sciences and Engineering Research Council (NSERC) of Canada.

[1] W. H. Furry, Phys. Rev. **51**, 125 (1937).
 [2] E. Wichmann and N. M. Kroll, Phys. Rev. **96**, 232 (1954).
 [3] E. H. Wichmann and N. M. Kroll, Phys. Rev. **101**, 843 (1956).
 [4] M. Eides, H. Grotch, and V. Shelyuto, *Theory of Light Hydrogenic Bound States*, Springer Tracts in Modern Physics (Springer, Berlin, 2007).
 [5] M. I. Eides, H. Grotch, and D. A. Owen, Phys. Lett. **B294**, 115 (1992).
 [6] K. Pachucki, Phys. Rev. **A48**, 2609 (1993).
 [7] K. Pachucki, Phys. Rev. Lett. **72**, 3154 (1994).
 [8] M. Dowling, J. Mondéjar, J. H. Piclum, and A. Czarnecki, Phys. Rev. **A81**, 022509 (2010), arXiv:0911.4078 [hep-ph].
 [9] K. Melnikov and T. van Ritbergen, Phys. Rev. Lett. **84**, 1673 (2000), hep-ph/9911277.
 [10] U. D. Jentschura, A. Czarnecki, and K. Pachucki, Phys. Rev. **A72**, 062102 (2005).
 [11] A. Pineda and J. Soto, Phys. Lett. **B420**, 391 (1998), hep-ph/9711292.
 [12] R. J. Hill, G. Lee, G. Paz, and M. P. Solon, Phys. Rev. **D87**, 053017 (2013), arXiv:1212.4508 [hep-ph].
 [13] A. Czarnecki, U. D. Jentschura, and K. Pachucki, Phys. Rev. Lett. **95**, 180404 (2005).
 [14] C. G. Parthey *et al.*, Phys. Rev. Lett. **107**, 203001 (2011), arXiv:1107.3101 [physics.atom-ph].
 [15] M. Herrmann, M. Haas, U. D. Jentschura, F. Kottmann, D. Leibfried, G. Saathoff, C. Gohle, A. Ozawa, V. Battieger, S. Knünz, N. Kolachevsky, H. A. Schüssler, T. W. Hänsch, and T. Udem, Phys. Rev. A **79**, 052505 (2009).
 [16] R. K. Altmann, S. Galtier, L. S. Dreissen, and K. S. E. Eikema, Phys. Rev. Lett. **117**, 173201 (2016).
 [17] K. Pachucki, Phys. Rev. **A63**, 042503 (2001).
 [18] K. Pachucki, A. Czarnecki, U. D. Jentschura, and V. A. Yerokhin, Phys. Rev. A **72**, 022108 (2005), physics/0506227.
 [19] S. Sturm, F. Köhler, J. Zatorski, A. Wagner, Z. Harman, G. Werth, W. Quint, C. H. Keitel, and K. Blaum, Nature **506**, 467 (2014).
 [20] S. G. Karshenboim and A. I. Milstein, Phys. Lett. **B549**, 321 (2002), arXiv:hep-ph/0210069 [hep-ph].
 [21] R. N. Lee, A. I. Milstein, I. S. Terekhov, and S. G. Karshenboim, Phys. Rev. **A71**, 052501 (2005), arXiv:hep-ph/0412026 [hep-ph].

- [22] N. A. Belov, B. Sikora, R. Weis, V. A. Yerokhin, S. Sturm, K. Blaum, C. H. Keitel, and Z. Harman, “Muonic vacuum polarization correction to the bound-electron g -factor,” (2016), arXiv:1610.01340v1 [physics.atom-ph].
- [23] R. Pohl, R. Gilman, G. A. Miller, and K. Pachucki, Ann. Rev. Nucl. Part. Sci. **63**, 175 (2013), arXiv:1301.0905 [physics.atom-ph].